Journal of Alloys and Compounds, 207/208 (1994) 83–86
JALCOM 3020

Non-resonant energy transfer from the $^5D_4$ level of Tb^{3+} to the $^5D_0$ level of Eu^{3+}

P.A. Tanner and Y.-L. Liu
Department of Biology and Chemistry, City Polytechnic of Hong Kong, Tat Chee Avenue, Kowloon (Hong Kong)

M. Chua
Department of Physics, University of Hong Kong, Pokfulam Road, Hong Kong (Hong Kong)

M.F. Reid
Departmemt of Physics and Astronomy, University of Canterbury, Christchurch (New Zealand)

Abstract

The infrared absorption spectrum and the visible emission spectra of $Cs_2NaTbCl_6$ are used to provide assignments for the energy levels of this cubic elpasolite system, up to 21 000 cm^{-1}. The spectra have been interpreted in detail, particularly with respect to the vibrational sidebands of the electronic transitions. Together with the measured oscillator strengths from the $^5D_0 \leftarrow {}^7F_0$ absorption spectrum of $Cs_2NaEuCl_6$, the data are used in a spectral overlap model to calculate the energy transfer rate from the $^5D_4$ term manifold of Tb^{3+} to the $^5D_0$ term of Eu at 77 K. The calculated rate is 1.4×10^6 times smaller than the previously reported [1] energy transfer rate, so that it appears unlikely that the $^5D_4$ luminescence quenching in $Cs_2NaTbCl_6$:$EuCl_6^{3-}$ is due to the proposed cross-relaxation mechanism.

---

1. Introduction

In this study, a calculation is presented of the rate of non-resonant energy transfer from Tb^{3+} to Eu^{3+} in the solid state elpasolite system $Cs_2NaTbCl_6$:$EuCl_6^{3-}$ at 77 K. This process has been attributed [1,2] to the cross-relaxation shown in Fig. 1. Interest in this problem was aroused from previous qualitative explanations in [1], because the quenching of the $^5D_4$ luminescence is efficient, yet the process in Fig. 1 involves two of the weakest optical transitions in the spectra of Tb^{3+} and Eu^{3+} in elpasolite lattices. Furthermore, the $^5D_4$ energy migration has been attributed to an electric quadrupole (EQ) mechanism [1]. In the present study, the latter point is not considered, but it is noted that the transitions involving the lower levels of $^5D_4$ and $^7F_0$ are EQ forbidden. However, the proposed mechanism of the $Tb^{3+} \rightarrow Eu^{3+}$ energy transfer process [1,2] is examined both experimentally and theoretically.

Previous studies of the vibronic spectra and of the energy levels of $Cs_2NaTbCl_6$ [3–5] and $Cs_2NaEuCl_6$ [6,7] do not provide a sufficiently reliable background for the investigation of energy transfer phenomena. Therefore, the ^7F_J crystal field levels of $Cs_2NaTbCl_6$ have been determined from the infrared absorption spectrum and a reinvestigation of the $^5D_4 \rightarrow {}^7F_J$ emission transitions of $Cs_2NaTbCl_6$ has also been carried out. The $^5D_0 \leftarrow {}^7F_0$ absorption transition of $Cs_2NaEuCl_6$ is also reported, together with the oscillator strengths of vibronic origins.

2. Experimental details

The preparation of polycrystalline samples of elpasolites followed the method E in [8]. Samples were then passed, in a sealed quartz tube, through a Bridgmann furnace at 850 °C. The spectrometers used in this study have been described in [9].

3. Results and discussion

3.1. *Energy levels and description of the energy transfer process*

The 20 K infrared spectrum of $Cs_2NaTbCl_6$ was recorded between 3000 and 7200 cm^{-1}, and all features were assigned to either (i) magnetic dipole (MD) origins; (ii) vibronic structure; and (iii) electric dipole (ED) transitions of Tb^{3+} ions situated at defect sites, in the

0925-8388/94/$07.00
SSDI 0925-8388(93)03020-J

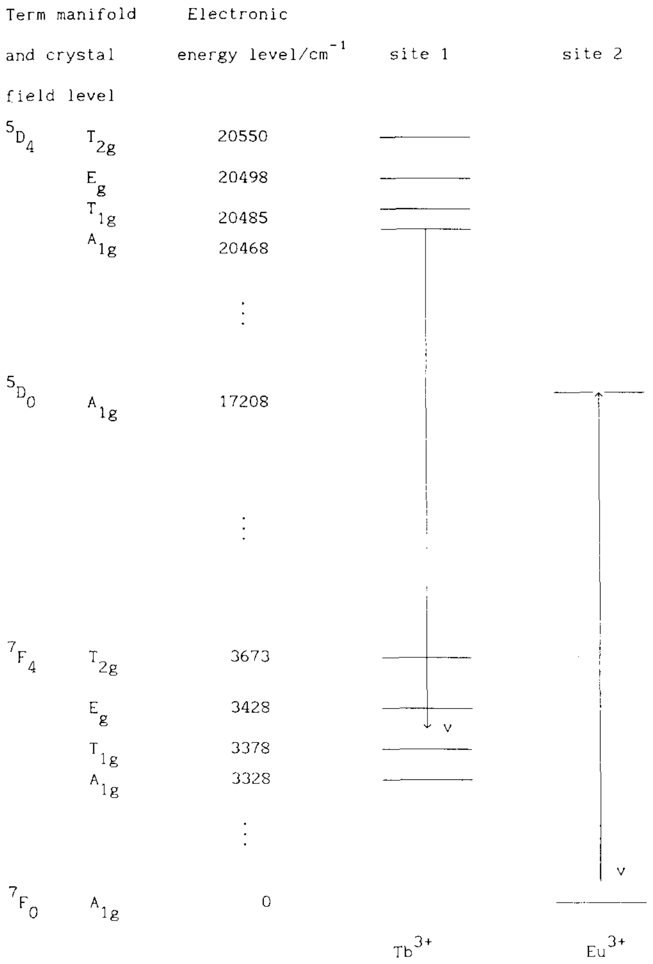

Fig. 1. Proposed ion-ion cross-relaxation mechanism responsible for the quenching of Tb^{3+} emission in $Cs_2NaTbCl_6$:$EuCl_6^{3-}$. Note that the diagram is not to scale, and only the term manifolds in the cross-relaxation are shown. Refer to Table 1 for the energies of other Tb^{3+} levels. v denotes a transition terminating in or originating from a vibronic level.

TABLE 1. Crystal field levels of $Cs_2NaTbCl_6$ derived from the 20 K infrared absorption and visible luminescence spectra

Multiplet crystal field Term	Level	Energy (cm^{-1}) From absorption	From $^5D_4$ emission
$^7F_6$	A_{1g}	0	0
	T_{1g}	–	36
	aT_{2g}	–	75
	bT_{2g}	–	356
$^7F_5$	aT_{1g}	–	2084±1
	T_{2g}	–	2246.5±0.5
	E_g	–	2318.5±0.5
	bT_{1g}	–	2349
$^7F_4$	A_{1g}	3330	3328
	T_{1g}	(3378)	3377.5±0.5
	E_g	3428	3428
	T_{2g}	3673	3672
$^7F_3$	T_{1g}	4411	4411
	T_{2g}	4445	4445
	A_{2g}	4557	4557
$^7F_2$	T_{2g}	5110	5109
	E_g	5300	5299
$^7F_1$	T_{1g}	5619	5618
$^7F_0$	A_{1g}	5838	–
$^5D_4$	A_{1g}	–	20468±2
	T_{1g}	–	20485±2
	E_g	–	20498±2
	T_{2g}	–	20550±2

From the infrared spectrum, the error in location is ±1 cm^{-1} for directly observed zero phonon lines, and ±2 cm^{-1} for origins inferred from vibronic structure. Unless otherwise stated, the error in location from emission is ±2 cm^{-1}.

TABLE 2. Oscillator strengths of bands in the 15 K $(^5D_0)A_{1g} \leftarrow A_{1g}(^7F_0)$ absorption spectrum of $Cs_2NaEuCl_6$

Wavenumber (cm^{-1})	Oscillator strength (10^{-10})	Assignment for terminal $^5D_0$ level[a]
17306	3.19	S_7(TO)
17331	1.44	S_7(TO); S_4(ZB)
17386	1.81	S_8
17443	0.34	S_6(ZB); S_2(ZB)
17460	0.67	S_6(TO)
17490	1.60	S_6(LO); S_1(ZB)

[a] The initial level is $^7F_0$ in all cases. The vibrational notation is that of Lentz [10]. The FWHM of bands is 11 cm^{-1}.

case of some weak bands. In this spectral region, 11 electronic transitions were observed, and each one exhibited a well-resolved sideband. The assignment of vibronic structure is illustrated for the τ_{1u} vibrational sideband of $(^7F_0)A_{1g} \leftarrow A_{1g}(^7F_6)$ in Fig. 2. The τ_{2u} vibrational mode is forbidden, to first order, in this transition, and appeared as a feature at 82 cm^{-1}, with a shoulder at 72 cm^{-1}, in other transitions. The assignments for the crystal field levels, from the infrared absorption and the visible emission are collected in Table 1.

Complete assignments have recently been given for the energy levels of Eu^{3+} in $Cs_2NaEuCl_6$, up to 21 500 cm^{-1} [9]. The oscillator strengths and assignments for features in the 15 K $^5D_0 \leftarrow {}^7F_0$ absorption spectrum are given in Table 2. The quenching of the $^5D_4$ Tb emission, in crystals also containing Eu, has been attributed to the phonon-assisted ion-ion cross-relaxation process shown in Fig. 1 [1,2]. In the case of $Cs_2NaTbCl_6$:$EuCl_6^{3-}$, an understanding of the $^5D_4 \rightarrow {}^7F_4$ emission transition is therefore required, in order to assess the spectral overlap with the $^5D_0 \leftarrow {}^7F_0$ transition of $Cs_2NaEuCl_6$. The interpretation of this emission transition is incorrect in previous studies [3,4]. In the present study, all spectral features in the 20 K spectrum have been assigned, and it is noted that some

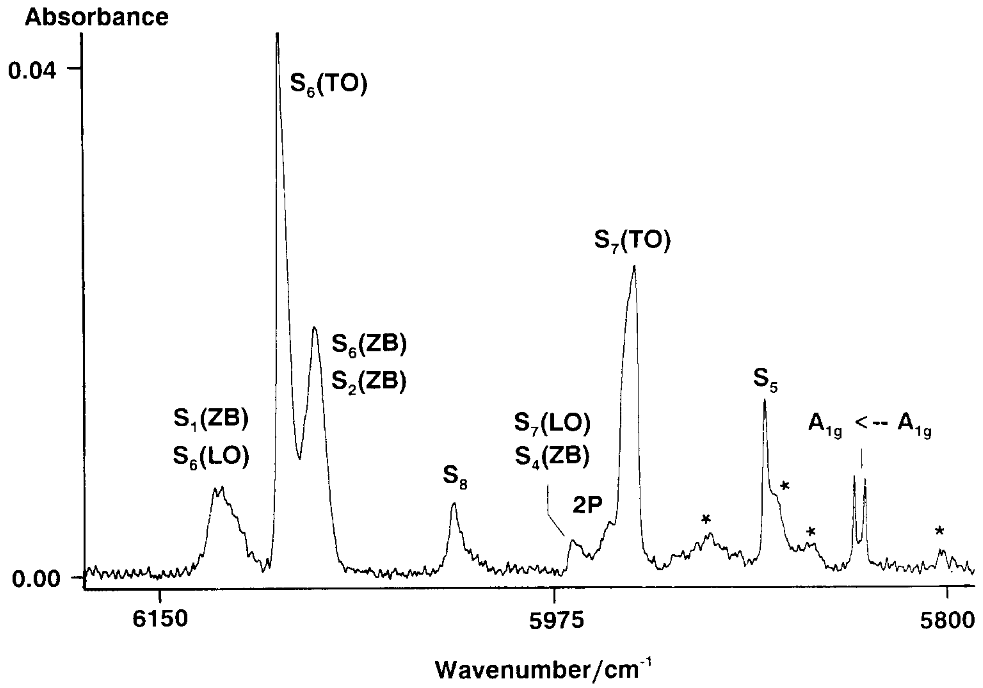

Fig. 2. 20 K absorption spectrum of $Cs_2NaTbCl_6$ between 5800 and 6150 cm^{-1}. Resolution 2 cm^{-1}. The vibrational notation is that of Lentz [10]. ZB, zone boundary; TO, transverse optic; LO, longitudinal optic; 2P, two phonon. Starred bands correspond to (overlapping) vibronic structure of the $(^7F_1)T_{1g} \leftarrow T_{1g}(^7F_6)$ transition.

of the strongest bands (lines 29, 32 in [3]) in the previously published spectra are not observed.

The major interest in this study concerns the spectral overlap of the $^5D_4 \rightarrow {}^7F_4$ and $^5D_0 \leftarrow {}^7F_0$ transitions. Above 77 K, the diffuseness of structure in these transitions does not enable the possible vibronic transfer mechanisms to be identified. However, this may be possible at, or below 77 K, because the transitions are more clearly resolved. The experimentally measured energy transfer rate from $Tb^{3+} \rightarrow Eu^{3+}$ decreases only by a factor of 2.1, from 293 K to 77 K [1]. Study of the 77 K spectra may thus enable the dominant energy transfer process to be identified.

Due to the energy mismatch, the overlap of the Eu^{3+} transition with the $^5D_4 \rightarrow {}^7F_4$ transition of Tb^{3+} must involve hot bands (*i.e.* ED vibronic origins) of the $^5D_0 \leftarrow {}^7F_0$ transition. At 77 K, the strongest of these is observed at 17 104 cm^{-1} (there are small wavenumber shifts with change in temperature), corresponding to $^5D_0 \leftarrow S_7(TO) + {}^7F_0$, for which the oscillator strength is calculated, from the data in Table 2, to be 5.3×10^{-11} at 77 K. The oscillator strengths of the corresponding hot bands involving the S_7(LO) and S_8 vibronic origins are calculated, from Table 2, to be 1.5×10^{-11} and 6.8×10^{-12}, respectively.

In the $^5D_4 \rightarrow {}^7F_4$ emission spectrum of $Cs_2NaTbCl_6$ at 20 K, the strongest feature occurs at 17 090 cm^{-1}. Bettinelli and Flint [1] have interpreted the 77 K $Tb^{3+} \rightarrow Eu^{3+}$ energy transfer process as involving this Tb^{3+} transition. However, our spectral assignments, together with the dipole calculations in [4], clearly identify the feature at 17 090 cm^{-1} as the $(^5D_4)A_{1g} \rightarrow T_{1g}(^7F_4)$ MD origin. The energy transfer rate for a process involving an ED transition at one site, and a MD transition at the other, is zero in this centrosymmetric system [11]. The only possible transfer routes must therefore involve the broader, weaker, coincident ED vibronic structure underlying this MD origin, and/or the weak structure which is at a similar wavenumber to the Eu^{3+} transitions $(^5D_0)A_{1g} \leftarrow S_8, S_7(LO) + A_{1g}(^7F_0)$. From the comparison with the (calculated) intensity of MD structure, we may estimate the oscillator strengths of these bands (FWHM *ca.* 20 cm^{-1}) in the 77 K $^5D_4 \rightarrow {}^7F_4$ emission spectrum. The magnitudes in each case are $< 1.67 \times 10^{-9}$, and this value is utilized in the calculation to give an upper-limit on the energy transfer rate.

3.2. Calculation of non-resonant $Tb^{3+} \rightarrow Eu^{3+}$ energy transfer rate

The $Tb^{3+} \rightarrow Eu^{3+}$ energy transfer rate in $Cs_2NaTb_{0.9}Eu_{0.1}Cl_6$ at 77 K has been calculated using a spectral overlap model, fully described in [12], for which the input data are the vibronic oscillator strengths of the donor and acceptor transitions. The spectral overlap of all hot bands of the $^5D_0 \leftarrow {}^7F_0$ Eu^{3+} transition with the vibronic structure of the $^5D_4 \rightarrow {}^7F_4$ Tb^{3+} transition was taken into account. The transfer rate to all nearest neighbours, up to the seventh distant shell, is calculated to be 1.6×10^{-4} s . The experimentally measured transfer rate is 228 s^{-1} [1].

4. Conclusions

In the conventional treatment of phonon-assisted energy transfer processes, the energy transfer rate is expressed as the product of two terms which are dependent, respectively, upon the electronic resonant transfer rate, and the properties of the phonons involved [13]. For the $Tb^{3+} \rightarrow Eu^{3+}$ energy transfer process shown in Fig. 1, the electronic term is negligible, since the transition line strengths are very small. Since the conventional model fails to account for the efficient energy transfer, an alternative approach which considers the non-radiative coupling of vibronic transitions at the Tb^{3+} and Eu^{3+} sites has been presented in this study. This spectral overlap model, however, leads to the result that the $Tb^{3+} \rightarrow Eu^{3+}$ transfer does not occur through the mechanism involving the non-radiative transitions shown in Fig. 1. The energy transfer rate is proportional to the product of the donor and acceptor oscillator strengths, and the product is more than 10^6 times too small to account for the transfer process by the route in Fig. 1. The spectral overlap occurs for moiety modes of relatively high energy (96 cm^{-1} or greater) and would not account for the observed temperature dependence of the energy transfer rate.

Alternative energy transfer mechanisms are possible, notably that involving the Eu^{3+} $^5D_1$ state, and more thorough low-temperature experimental investigation of the luminescence quenching in this doped elpasolite system is now being carried out.

Acknowledgment

P.A.T. and Y.-L.L. acknowledge financial support under HK UPGC RG nos. 904057 and 904022.

References

1 M. Bettinelli and C.D. Flint, *J. Phys.: Condensed Matter, 2* (1990) 8417.
2 I. Laulicht and S. Meirman, *J. Lumin., 34* (1986) 287.
3 L.C. Thompson, O.A. Serra, J.P. Riehl and F.S. Richardson, *Chem. Phys., 26* (1977) 393.
4 T.R. Faulkner and F.S. Richardson, *Mol. Phys., 36* (1978) 193.
5 R.W. Schwartz, H.G. Brittain, J.P. Riehl, W. Yeakel and F.S. Richardson, *Mol. Phys., 34* (1977) 361.
6 O.A. Serra, L.C. Thompson and J.A. Koningstein, *Chem. Phys. Lett., 46* (1977) 253.
7 C.D. Flint and F.L. Stewart-Darling, *Mol. Phys., 44* (1981) 61.
8 L.R. Morss, M. Siegel, L. Stenger and N. Edelstein, *Inorg. Chem., 9* (1970) 1771.
9 P.A. Tanner and Y.-L. Liu, *J. Alloys Comp.*, in press.
10 A. Lentz, *J. Phys. Chem. Solids, 35* (1974) 827.
11 M. Chua, P.A. Tanner and M.F. Reid, *Solid State Commun.*, in press.
12 M. Chua, P.A. Tanner and M.F. Reid, *J. Lumin.*, submitted for publication.
13 T. Holstein, S.K. Lyo and R. Orbach, in W.M. Yen and P.M. Selzer (eds.), *Laser Spectroscopy of Solids*, Springer, New York, 1981.